PROCEEDINGS OF SCIENCE

Studies of the mass composition of cosmic rays and proton-proton interaction cross-sections at ultra-high energies with the Pierre Auger Observatory

Olena Tkachenko[a,*] **for the Pierre Auger Collaboration**[b]

[a] *Karlsruhe Institute of Technology, Kaiserstraße 12, 76131 Karlsruhe, Germany*

[b] *Observatorio Pierre Auger, Av. San Martín Norte 304, 5613 Malargüe, Argentina*

Full author list: https://www.auger.org/archive/authors_icrc_2023.html

E-mail: spokespersons@auger.org

In this work, we present an estimate of the cosmic-ray mass composition from the distributions of the depth of the shower maximum ($X_{\max}$) measured by the fluorescence detector of the Pierre Auger Observatory. We discuss the sensitivity of the mass composition measurements to the uncertainties in the properties of the hadronic interactions, particularly in the predictions of the particle interaction cross-sections. For this purpose, we adjust the fractions of cosmic-ray mass groups to fit the data with $X_{\max}$ distributions from air shower simulations. We modify the proton-proton cross-sections at ultra-high energies, and the corresponding air shower simulations with rescaled nucleus-air cross-sections are obtained via Glauber theory. We compare the energy-dependent composition of ultra-high-energy cosmic rays obtained for the different extrapolations of the proton-proton cross-sections from low-energy accelerator data.

38th International Cosmic Ray Conference (ICRC2023)
26 July – 3 August, 2023
Nagoya, Japan

*Speaker

https://pos.sissa.it/

PoS(ICRC2023)438

1. Introduction

Knowledge of the primary composition of cosmic rays is very important for understanding the nature and origin of ultra-high-energy cosmic rays (UHECR). As cosmic rays propagate toward Earth, they interact with nuclei in the atmosphere producing cascades of secondary particles, also known as Extensive Air Showers (EAS). The atmospheric depth at which the particle shower reaches its maximum, $X_{\max}$, is one of the most sensitive observables to estimate the mass composition of UHECRs. By fitting the measured $X_{\max}$ distributions with the model predictions derived from air shower simulations, one can estimate the primary cosmic-ray mass composition at ultra-high energies [1]. However, prediction of the development of hadronic interactions in the atmosphere is difficult, and describing their properties above the LHC energies is a challenging task [2]. Since direct measurements at ultra-high energies are not yet experimentally feasible, our understanding of hadronic interactions in EAS relies on the extrapolations from accelerator data. The phenomenological hadronic interaction models, such as, for example, EPOS-LHC [3], QGSJETII-04 [4], and Sibyll 2.3d [5] are broadly used for the simulations of the development of the cosmic-ray air showers and provide a reasonably good overall description of hadronic showers. Yet, the interpretations of air shower observables remain an open question as they are sensitive to the systematic uncertainties in the modeling [6].

The Pierre Auger Observatory, located near Malargüe in Argentina, is the largest observatory to measure the most energetic cosmic ray particles. The hybrid design of the Observatory provides two independent and complementary approaches for the detection of cosmic rays. The Surface Detector array consists of more than 1600 water-Cherenkov detectors and measures the cosmic ray particles at the ground level. The fluorescence telescopes measure the development of the longitudinal profile of the electromagnetic cascade in the atmosphere.

In this work, we present an update on the estimation of the primary mass composition from the maximum of the air shower development profile as measured by the Fluorescence Detectors of the Pierre Auger Observatory. We study and discuss the sensitivity of the obtained composition fractions to the underlying proton-proton and, more broadly, nucleus-air interaction cross-sections.

2. Measurement of the cosmic-ray mass composition

To derive the cosmic-ray mass composition, we follow a standard approach and fit the $X_{\max}$ distributions with the model predictions obtained from the air shower simulations with the Conex [7] program, and EPOS-LHC and Sibyll 2.3d hadronic interaction models. We omit the QGSJETII-04 interaction model since it does not describe the $X_{\max}$ distributions well [8]. We use a binned maximum likelihood fit, and the goodness of the fit is characterized by the p-value, calculated as a probability of getting a worse fit with the predicted $X_{\max}$ distributions than with the actual data. The $X_{\max}$ resolution and acceptance were simulated according to their parameterizations provided in the detailed study on the $X_{\max}$ distributions in [9] and updated for the most recent data in [10]. The fit was performed using the Markov Chain Monte Carlo (MCMC) inference approach [11], which has several advantages compared to the frequentist inference. Firstly, MCMC can be applied to global optimization problems, and it will not get stuck in a local minimum (at least theoretically, if the number of samples is infinite and/or the sampling steps are set appropriately). More importantly, it

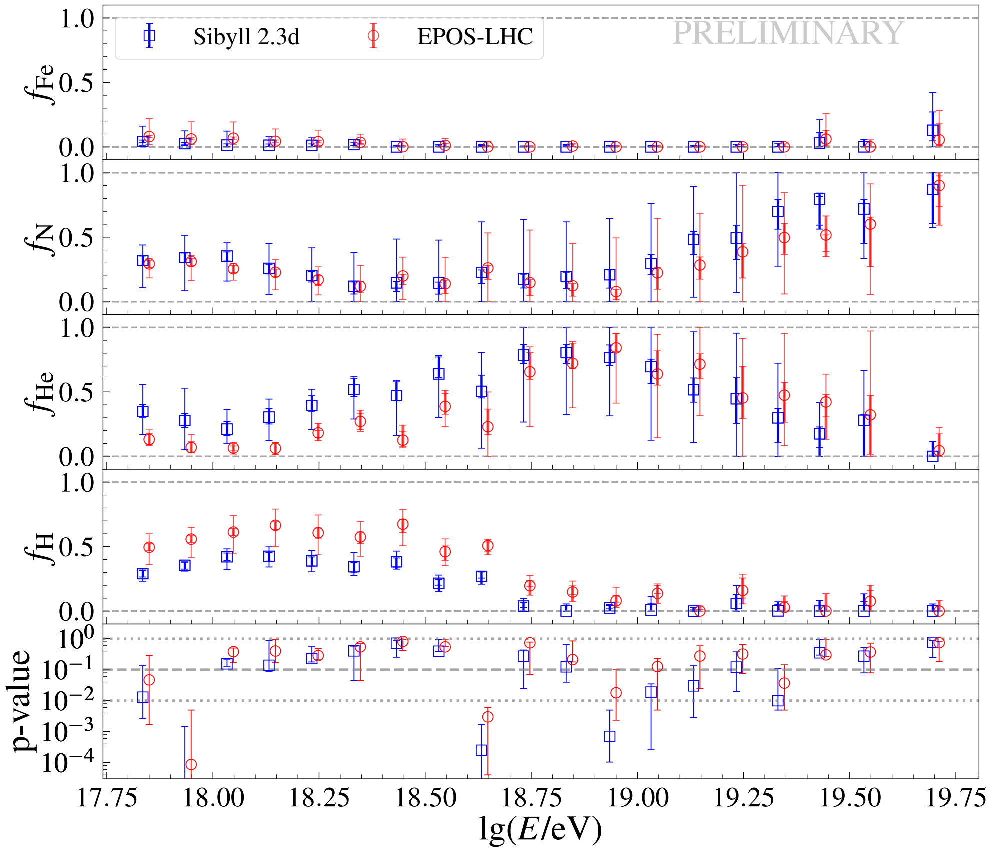

Figure 1: The mass composition fit for four elemental mass groups (top four panels). The error bars denote statistical (inner cap) and total (outer cap) uncertainties. The bottom panel shows the *p*-values of the fit.

allows sampling the posterior probability density function of the estimated fractions making it easy to marginalize over the mass composition for derived quantities, e.g., the first moments of the X_{max} distribution. Furthermore, MCMC can deal with many highly correlated parameters, numerically impossible with standard gradient minimizers. This can be very useful for composition studies if, in addition to the nuclear fractions, one also wishes to fit properties of hadronic interactions.

In Fig.1, the mass composition fit is shown for a combination of four particle species: proton, H; Helium, He; Nitrogen, N, and Iron, Fe, representing four elemental groups, approximately equally spaced in $\ln A$. The total uncertainty on the composition fractions includes the statistical uncertainty from the MCMC posterior distributions and the impact of the systematic uncertainty on the X_{max} scale, evaluated by fitting the data with a consistently varied shift in the X_{max} within the scale uncertainty. The trends observed in the evolution of the cosmic ray composition with energy agree with our previous results presented in [1, 8]. Minor differences from the previous results in the individual mass groups are likely attributed to the larger dataset (more observation years) and the usage of the most recent version of the Sibyll interaction model, which predicts slightly shallower showers than the previous one [5]. Though the qualitative behavior is the same, one can also see the significant dependence of the choice of the interaction model on the individual fractions. On average, the Sibyll 2.3d interaction model results in a He fraction that is ≈ 20% larger at lower energies and in an increase of the fraction of N nuclei at higher energies compared to EPOS-LHC.

Overall, the composition is a mix of H, He, and N nuclei at lower energies and dominated by He and N at higher energies. The proton fraction obtained with EPOS-LHC reaches up to 70% around $10^{18.0}$ - $10^{18.2}$ eV and then drops to less than 20% above $10^{18.7}$ eV. The Sibyll 2.3d predicts a smaller proton fraction over the energy range considered, with a near-zero contribution at the higher energies. The amount of iron in the cosmic-ray mix is consistent with zero within uncertainties at all energies. Within the energy range observed, the data is compatible with a cycle from H to He to N; see [12] for further discussion in the astriophysical context.

3. Modifying the proton-proton interaction cross-sections

To study the effect of the uncertainties in the extrapolated characteristics of the hadronic interactions on the measurements of the primary cosmic-ray mass composition at ultra-high energies, we perform a mass composition fit described above with model predictions constructed under the assumption of altered proton-proton interactions. For this, we follow an approach for varying the proton-proton interaction cross-sections, discussed in [13], with a subsequent self-consistent rescaling of the cross-sections modifications into the nucleus-nucleus interaction via the Glauber [14] theory. We multiply the original cross-sections by an energy-dependent scaling factor [6]:

$$f(E) = 1 + H(E - E_0)(f_{\lg E_1} - 1)\frac{\lg(E/E_0)}{\lg(E_1/E_0)}, \qquad (1)$$

where E_0 and E are the threshold energy and the energy of interest respectively, $f_{\lg E_1}$ is the rescaling factor at $E = E_1$, and $H(x)$ denotes the Heaviside step function. Since we use the LHC center-of-mass energy of $\sqrt{s}$ = 14 TeV as a threshold energy, the scaling factor equals unity at the lower energies. We also keep E_1 equal to 10^{19} eV, so $f(E)$ is equal to $f_{\lg E_1=19}$ at this energy. Rather than changing the $f(E)$, we vary the energy-independent f_{19}, which we refer to as the scaling factor below.

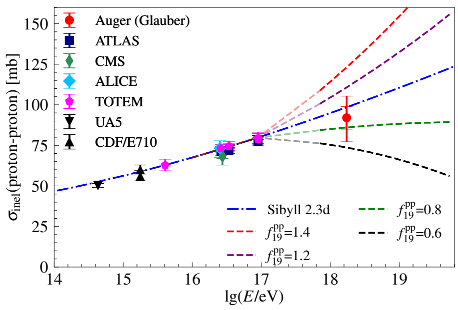

Figure 2: Comparison of the measured σ^{pp} with model extrapolations.

In Fig.2, we show how much of the deviation in the inelastic proton-proton cross-sections is expected when the rescaling is applied to the most recent Sibyll 2.3d interaction model. For comparison, we also show the accelerator-based measurements (see for reference [16]-[21]), and the measurement at the $\sqrt{s}$=57 TeV with the Pierre Auger Observatory [22]. The estimated proton-proton cross sections from the cosmic ray data agree with the range of scaling factor values between 0.7 and 1.2 within the uncertainties.

4. Implications of the proton-proton cross-section extrapolation for the estimation of the mass composition

To estimate how the properties of the hadronic interaction models, in this particular study, the changes in the proton-proton cross-sections, affect the measured mass composition of cosmic rays, we have varied the introduced rescaling factor in a wide range of values. To generate the

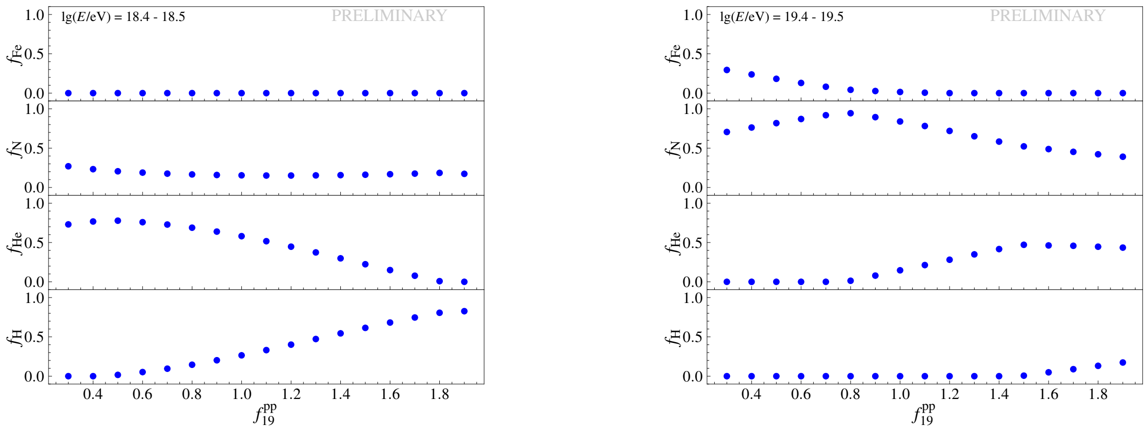

Figure 3: Composition estimates for the varied f_{19}^{pp} for $10^{18.4}$-$10^{18.5}$ eV (left) and $10^{19.4}$-$10^{19.5}$ eV (right).

X_{max} distribution templates for the narrowly spaced scaling factors more efficiently, we use the generalized Gumbel distribution [15] with shape parameters having a functional dependence on the scaling factor values instead of performing air shower simulations for each f_{19}^{pp}. The modifications in the interaction cross-section will affect the EAS observables, and, as of interest in this study, an increase in the scaling factor makes the X_{max} distributions shallower and narrower. In Fig.3, an example of how much the fitted composition changes with variations in the input rescaling factor is shown. On the left plot, the fit is shown for the intermediate energies of $10^{18.4}$ - $10^{18.5}$ eV, where lighter nuclei with a small contribution dominate the fit. Given the onset of the proton-proton cross-section modifications at the LHC center-of-mass energy, the iron-air interactions are unaffected at these energies, so we expect it to remain stable. The changes in the nitrogen fraction are also very subtle, except for the rescaling factor values corresponding to the unrealistically small interaction cross-sections. The proton and helium fractions are, indeed, sensitive to the variations in the rescaling factor, and the composition spans the range from being dominant by He nuclei at smaller f_{19}^{pp} values to being dominant by protons. In the right panel, a fit is shown for the higher energies ($10^{19.4}$ - $10^{19.5}$ eV), where the composition is a mix of heavier nuclei. With an increase in the scaling factor, the composition is getting lighter.

The overall mass composition behavior with a variation in the rescaling factor is shown in Fig.4. For the clarity of the comparison, we do not show the uncertainties on composition fraction fitted under the assumption of the modified cross-sections as all fits use the same data, and the error bars are very similar for each scaling factor. At lower energies, where the composition is characterized by a combination of three particle species (H, He, and N), the most noticeable difference occurs for H and He fractions. Here, the increase in the scaling factor, and therefore, in the interaction cross-sections, leads to the increase in the proton fraction and in the corresponding decrease in the amount of He. Although nitrogen interactions already change at around $10^{18.1}$ eV, there is no discernible effect until $10^{18.7}$ eV, where there is a drop in the detected number of protons. Beyond this point, since the proton fraction makes up less than 5%, the main change in the composition is observed for He and N nuclei. The same pattern as for the lower energies, with an increase in the fraction of the lighter nuclei for the larger scaling factors, is also seen at the higher energies. Furthermore, in the energy range above $10^{18.7}$ eV, the deviation from the default mass composition fit increases with energy for He and N nuclei. Except for a few energies where it does contribute to

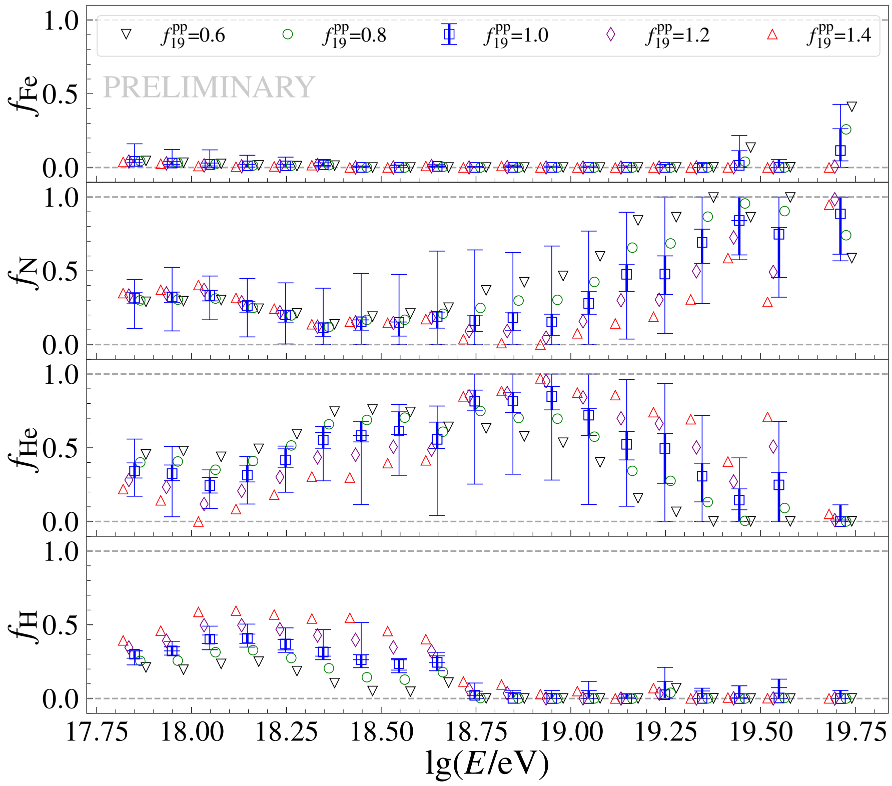

Figure 4: Mass composition fit for the different extrapolations of the proton-proton cross-section.

the fit, the iron fraction remains stable. For the two energy bins where the fitted iron fraction rises above 0, the increase in the f_{19}^{pp} results in the decrease of the corresponding fraction. Additionally, the presence of the iron nuclei in the composition mix makes other particle species less sensitive to the modifications in the interaction cross-sections. There is no significant dependence from the scaling factor's variation on the fit quality at each energy. An example of the X_{max} distributions fits from the air shower simulations with modified proton-proton cross-section is shown in Fig.5. As can be seen, increasing f_{19}^{pp} from 0.8 to 1.2 reduces the He fraction from $\approx$ 0.7 to 0.4, and the contribution from H grows. However, the mean and dispersion of the total distribution remain constant, and the changes in goodness of fit are minor.

In Fig.6, the first X_{max} distribution moments, mean $\langle X_{\mathrm{max}}\rangle$ (left) and $\sigma(X_{\mathrm{max}})$ (center), derived from the fractions [23] with varied rescaling factor, are shown with a comparison to the moments from X_{max} data [10]. Throughout the energy range, the mean $\langle X_{\mathrm{max}}\rangle$ remains stable irrespective of the interaction cross-section changes and agrees well with the data. Over almost the entire energy range, the mean $\langle X_{\mathrm{max}}\rangle$ varies only within a few g/cm^2, except for the highest energies, where the difference increases. In general, the standard deviation $\sigma(X_{\mathrm{max}})$ is getting smaller with an increase in the scaling factor. It is more affected by the rescaling in the cross-sections, particularly at energies above $10^{18.5}$ eV, reaching up to 10% deviation for the 20% variation in σ_{pp}. This trend is consistent with a lighter composition obtained from the fit associated with the larger cross-section values since both an increase in the scaling factor and an increase in the fraction of lighter nuclei have the same effect on the X_{max} distribution, narrowing it. On average, there is a good agreement between the calculated $\sigma(X_{\mathrm{max}})$ and the data, except for several energies where neither of the calculated second

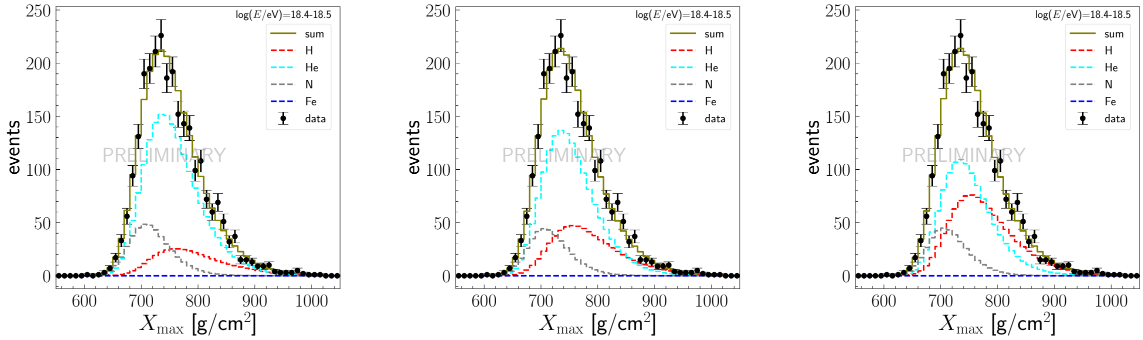

Figure 5: The fitted X_{max} distributions for the scaling factor values of 0.8 (left), 1.0 (center), and 1.2 (right).

moments provides a good interpretation.

In Fig.6 (right), the changes in the attenuation length Λ_η are shown with a comparison to data. The attenuation length is derived by fitting the tail of the X_{max} distribution, which can be described with an exponential profile $dN/dX_{\mathrm{max}} \propto \exp(-X_{\mathrm{max}}/\Lambda_\eta)$, where η is the fraction of the most deeply penetrating air showers considered for the fit. We select events in the tail of the X_{max} distribution following the previous analyses from the Pierre Auger Observatory with $\eta = 20\%$ [22]. The Λ_η is highly sensitive to the particle interactions in EAS and could be converted into the proton-air interaction cross-sections. The selection of the events in the tail enhances the contribution of protons. In this case, the estimation of the cross-sections is done under the assumption of a proton-dominated composition, with the possible contamination by helium nuclei being the largest source of the systematic uncertainty for the measurements of the proton-air cross-sections at ultra-high energies from the cosmic-ray data. See [22, 24] and [25, 26] for the previous results from the Pierre Auger Observatory and the Telescope Array, respectively.

We calculated the attenuation length values for the different values of the scaling factor from the X_{max} distributions corresponding to the fitted composition. With an increase in energy, the size of the selected sample decreases, leading to a larger uncertainty on the estimation of Λ_η from the data. Therefore, we show only the limited energy range, where it is still possible to estimate Λ_η with reasonably good accuracy without increasing the size of energy bins. The dependence of the Λ_η on the scaling factor is similar to the one observed for the $\sigma(X_{\mathrm{max}})$ - with an increase in the scaling factor (and, therefore, for larger proton-proton cross-sections) Λ_η is getting smaller. While the dependence on the scaling factor is not strong for lower energies, the difference between the results for different scaling factors increases at larger energies. The attenuation length values calculated under the assumption of the fitted composition agree well with the data.

5. Conclusions

In this contribution, we presented an update on the measurements of the cosmic-ray mass composition using the data from Pierre Auger Observatory. To estimate the effect of the uncertainties in the characteristics of the hadronic interactions, we tested the stability of the mass composition fit with respect to the changes in the proton-proton cross-sections.

The mass composition of cosmic rays is dominated by lighter elements at lower energies and a heavier mix at higher energies. The observed qualitative behavior of changes in mass composition

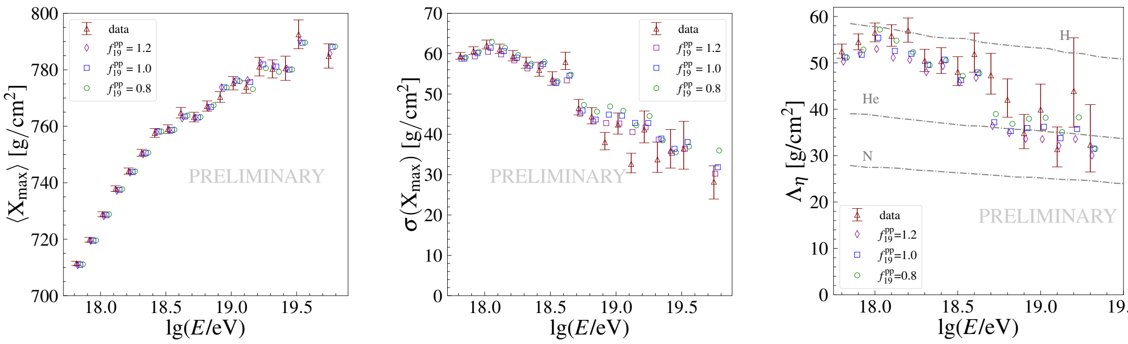

Figure 6: The first two moments of the X_{max} distribution, mean $\langle X_{max}\rangle$ (left) and standard deviation $\sigma(X_{max})$ (center), and the attenuation length Λ_η (right) derived from the measured composition fractions.

with energy is independent of cross-section extrapolation. The individual mass groups are, however, sensitive to the modifications in particle interactions. We see a small deviation from the default values in the fitted fractions for the proton-proton cross-section staying within the uncertainties of the current measurements from cosmic-ray data (± 20%). More significant variations substantially change the predictions from a nearly pure composition to a mix dominated by another nucleus. At high energies (above $10^{18.7}$ eV), significant anticorrelated changes for intermediate masses (He and N) of up to $\Delta f = 0.5$ can be seen. These changes are, however, within the systematic range of the X_{max} scale uncertainty. At lower energies, where the default proton fraction is significant, a change in σ_{pp} changes the proton fraction by up to ± 0.25 for very large changes in σ_{pp} of ± 40%. In further studies, we will explore if the shape of the X_{max} distribution provides enough sensitivity to fit the composition and cross-section simultaneously, as suggested in [13].

References

[1] A. Aab *et al.* [Pierre Auger Collaboration], *Phys. Rev. D* **90** (2014) 122006.

[2] R. Engel, H. Dieter, and T. Pierog, *Annu. Rev. Nucl. Part-Sci.* **61** (2011) 467.

[3] T. Pierog *et al.*, *Phys. Rev. C* **92** (2015) 034906.

[4] S. Ostapchenko, *Phys. Rev. D* **102** (2020) 063002.

[5] F. Riehn *et al.*, *Phys. Rev. D* **83** (2011) 014018.

[6] R. Ulrich, R. Engel, and M. Unger, *Phys. Rev. D* **83** (2011) 054026.

[7] T. Bergmann *et al.*, *Astropart. Phys.* **26** (2007) 420.

[8] J. Bellido for the Pierre Auger Collaboration, *PoS ICRC2017* (2017) 506.

[9] A.Aab *et al.* [Pierre Auger Collaboration], *Phys. Rev. D* **90** (2014) 122005.

[10] T. Fitoussi for the Pierre Auger Collaboration, *PoS ICRC2023* (2023) 319.

[11] D. W. Hogg and D. Foreman-Mackey, *ApJS* **236** (2018) 11.

[12] A. A. Halim *et al.* [Pierre Auger Collaboration], JCAP **05** (2023) 024.

[13] O. Tkachenko *et al.*, *PoS ICRC2021* (2021) 438.

[14] R.J. Glauber and G. Matthiae, *Nuclear Physics B* **21** (1970) 135.

[15] M. De Domenico, M. Settimo, S. Riggi and E. Bertin, JCAP **07** (2013), 050

[16] A. Amos *et al.*, *Phys.Rev.Lett.* **68** (1992) 2433.

[17] F. Abe *et al.*, *Phys.Rev.D* **50** (1994) 5550.

[18] G. Antchev *et al.* [TOTEM Collaboration], *Eur.Phys.J.C* **79** (2019) 861.

[19] B. Abelev *et al.* [ALICE Collaboration], *Eur.Phys.J.C* **73** (2013) 2456.

[20] CMS Collaboration, *JHEP* **07** (2018) 161.

[21] ATLAS Collaboration *Phys. Rev. Lett,* **117** (2016) 82002.

[22] P. Abreu *et al.* [Pierre Auger Collaboration], *Phys. Rev. Lett.* **109** (2012) 062002.

[23] P. Abreu *et al.* [Pierre Auger Collaboration] *JCAP* **02** (2013) 26.

[24] R. Ulrich for the Pierre Auger Collaboration, *PoS ICRC2015* (2015) 401.

[25] R.U. Abbasi *et al.* [Telescope Array Collaboration], *Phys. Rev. D* **92** (2015) 032007.

[26] R.U. Abbasi *et al.* [Telescope Array Collaboration], *Phys. Rev. D* **102** (2020) 062004.

The Pierre Auger Collaboration

A. Abdul Halim[13], P. Abreu[72], M. Aglietta[54,52], I. Allekotte[1], K. Almeida Cheminant[70], A. Almela[7,12], R. Aloisio[45,46], J. Alvarez-Muñiz[79], J. Ammerman Yebra[79], G.A. Anastasi[54,52], L. Anchordoqui[86], B. Andrada[7], S. Andringa[72], C. Aramo[50], P.R. Araújo Ferreira[42], E. Arnone[63,52], J. C. Arteaga Velázquez[67], H. Asorey[7], P. Assis[72], G. Avila[11], E. Avocone[57,46], A.M. Badescu[75], A. Bakalova[32], A. Balaceanu[73], F. Barbato[45,46], A. Bartz Mocellin[85], J.A. Bellido[13,69], C. Berat[36], M.E. Bertaina[63,52], G. Bhatta[70], M. Bianciotto[63,52], P.L. Biermann[h], V. Binet[5], K. Bismark[39,7], T. Bister[80,81], J. Biteau[37], J. Blazek[32], C. Bleve[36], J. Blümer[41], M. Boháčová[32], D. Boncioli[57,46], C. Bonifazi[8,26], L. Bonneau Arbeletche[21], N. Borodai[70], J. Brack[j], P.G. Brichetto Orchera[7], F.L. Briechle[42], A. Bueno[78], S. Buitink[15], M. Buscemi[47,61], M. Büsken[39,7], A. Bwembya[80,81], K.S. Caballero-Mora[66], S. Cabana-Freire[79], L. Caccianiga[59,49], I. Caracas[38], R. Caruso[58,47], A. Castellina[54,52], F. Catalani[18], G. Cataldi[48], L. Cazon[79], M. Cerda[10], A. Cermenati[45,46], J.A. Chinellato[21], J. Chudoba[32], L. Chytka[33], R.W. Clay[13], A.C. Cobos Cerutti[6], R. Colalillo[60,50], A. Coleman[90], M.R. Coluccia[48], R. Conceição[72], A. Condorelli[37], G. Consolati[49,55], M. Conte[56,48], F. Convenga[41], D. Correia dos Santos[28], P.J. Costa[72], C.E. Covault[84], M. Cristinziani[44], C.S. Cruz Sanchez[3], S. Dasso[4,2], K. Daumiller[41], B.R. Dawson[13], R.M. de Almeida[28], J. de Jesús[7,41], S.J. de Jong[80,81], J.R.T. de Mello Neto[26,27], I. De Mitri[45,46], J. de Oliveira[17], D. de Oliveira Franco[21], F. de Palma[56,48], V. de Souza[19], E. De Vito[56,48], A. Del Popolo[58,47], O. Deligny[34], N. Denner[32], L. Deval[41,7], A. di Matteo[52], M. Dobre[73], C. Dobrigkeit[21], J.C. D'Olivo[68], L.M. Domingues Mendes[72], J.C. dos Anjos, R.C. dos Anjos[25], J. Ebr[32], F. Ellwanger[41], M. Emam[80,81], R. Engel[39,41], I. Epicoco[56,48], M. Erdmann[42], A. Etchegoyen[7,12], C. Evoli[45,46], H. Falcke[80,82,81], J. Farmer[89], G. Farrar[88], A.C. Fauth[21], N. Fazzini[e], F. Feldbusch[40], F. Fenu[41,d], A. Fernandes[72], B. Fick[87], J.M. Figueira[7], A. Filipčič[77,76], T. Fitoussi[41], B. Flaggs[90], T. Fodran[80], T. Fujii[89,f], A. Fuster[7,12], C. Galea[80], C. Galelli[59,49], B. García[6], C. Gaudu[38], H. Gemmeke[40], F. Gesualdi[7,41], A. Gherghel-Lascu[73], P.L. Ghia[34], U. Giaccari[48], M. Giammarchi[49], J. Glombitza[42,g], F. Gobbi[10], F. Gollan[7], G. Golup[1], M. Gómez Berisso[1], P.F. Gómez Vitale[11], J.P. Gongora[11], J.M. González[1], N. González[7], I. Goos[1], D. Góra[70], A. Gorgi[54,52], M. Gottowik[79], T.D. Grubb[13], F. Guarino[60,50], G.P. Guedes[22], E. Guido[44], S. Hahn[39], P. Hamal[32], M.R. Hampel[7], P. Hansen[3], D. Harari[1], V.M. Harvey[13], A. Haungs[41], T. Hebbeker[42], C. Hojvat[e], J.R. Hörandel[80,81], P. Horvath[33], M. Hrabovský[33], T. Huege[41,15], A. Insolia[58,47], P.G. Isar[74], P. Janecek[32], J.A. Johnsen[85], J. Jurysek[32], A. Kääpä[38], K.H. Kampert[38], B. Keilhauer[41], A. Khakurdikar[80], V.V. Kizakke Covilakam[7,41], H.O. Klages[41], M. Kleifges[40], F. Knapp[39], N. Kunka[40], B.L. Lago[16], N. Langner[42], M.A. Leigui de Oliveira[24], Y Lema-Capeans[79], V. Lenok[39], A. Letessier-Selvon[35], I. Lhenry-Yvon[34], D. Lo Presti[58,47], L. Lopes[72], L. Lu[91], Q. Luce[39], J.P. Lundquist[76], A. Machado Payeras[21], M. Majercakova[32], D. Mandat[32], B.C. Manning[13], P. Mantsch[e], S. Marafico[34], F.M. Mariani[59,49], A.G. Mariazzi[3], I.C. Mariş[14], G. Marsella[61,47], D. Martello[56,48], S. Martinelli[41,7], O. Martínez Bravo[64], M.A. Martins[79], M. Mastrodicasa[57,46], H.J. Mathes[41], J. Matthews[a], G. Matthiae[62,51], E. Mayotte[85,38], S. Mayotte[85], P.O. Mazur[e], G. Medina-Tanco[68], J. Meinert[38], D. Melo[7], A. Menshikov[40], C. Merx[41], S. Michal[33], M.I. Micheletti[5], L. Miramonti[59,49], S. Mollerach[1], F. Montanet[36], L. Morejon[38], C. Morello[54,52], A.L. Müller[32], K. Mulrey[80,81], R. Mussa[52], M. Muzio[88], W.M. Namasaka[38], S. Negi[32], L. Nellen[68], K. Nguyen[87], G. Nicora[9], M. Niculescu-Oglinzanu[73], M. Niechciol[44], D. Nitz[87], D. Nosek[31], V. Novotny[31], L. Nožka[33], A Nucita[56,48], L.A. Núñez[30], C. Oliveira[19], M. Palatka[32], J. Pallotta[9], S. Panja[32], G. Parente[79], T. Paulsen[38], J. Pawlowsky[38], M. Pech[32], J. Pękala[70], R. Pelayo[65], L.A.S. Pereira[23], E.E. Pereira Martins[39,7], J. Perez Armand[20], C. Pérez Bertolli[7,41], L. Perrone[56,48], S. Petrera[45,46], C. Petrucci[57,46], T. Pierog[41], M. Pimenta[72], M. Platino[7], B. Pont[80], M. Pothast[81,80], M. Pourmohammad Shahvar[61,47], P. Privitera[89], M. Prouza[32], A. Puyleart[87], S. Querchfeld[38], J. Rautenberg[38], D. Ravignani[7], M. Reininghaus[39], J. Ridky[32], F. Riehn[79], M. Risse[44], V. Rizi[57,46], W. Rodrigues de Carvalho[80], E. Rodriguez[7,41], J. Rodriguez Rojo[11], M.J. Roncoroni[7], S. Rossoni[43], M. Roth[41], E. Roulet[1], A.C. Rovero[4], P. Ruehl[44], A. Saftoiu[73], M. Saharan[80], F. Salamida[57,46], H. Salazar[64], G. Salina[51], J.D. Sanabria Gomez[30], F. Sánchez[7], E.M. Santos[20], E. Santos[32],

F. Sarazin[85], R. Sarmento[72], R. Sato[11], P. Savina[91], C.M. Schäfer[41], V. Scherini[56,48], H. Schieler[41], M. Schimassek[34], M. Schimp[38], F. Schlüter[41], D. Schmidt[39], O. Scholten[15,i], H. Schoorlemmer[80,81], P. Schovánek[32], F.G. Schröder[90,41], J. Schulte[42], T. Schulz[41], S.J. Sciutto[3], M. Scornavacche[7,41], A. Segreto[53,47], S. Sehgal[38], S.U. Shivashankara[76], G. Sigl[43], G. Silli[7], O. Sima[73,b], F. Simon[40], R. Smau[73], R. Šmída[89], P. Sommers[k], J.F. Soriano[86], R. Squartini[10], M. Stadelmaier[32], D. Stanca[73], S. Stanič[76], J. Stasielak[70], P. Stassi[36], S. Strähnz[39], M. Straub[42], M. Suárez-Durán[14], T. Suomijärvi[37], A.D. Supanitsky[7], Z. Svozilikova[32], Z. Szadkowski[71], A. Tapia[29], C. Taricco[63,52], C. Timmermans[81,80], O. Tkachenko[41], P. Tobiska[32], C.J. Todero Peixoto[18], B. Tomé[72], Z. Torrès[36], A. Travaini[10], P. Travnicek[32], C. Trimarelli[57,46], M. Tueros[3], M. Unger[41], L. Vaclavek[33], M. Vacula[33], J.F. Valdés Galicia[68], L. Valore[60,50], E. Varela[64], A. Vásquez-Ramírez[30], D. Veberič[41], C. Ventura[27], I.D. Vergara Quispe[3], V. Verzi[51], J. Vicha[32], J. Vink[83], J. Vlastimil[32], S. Vorobiov[76], C. Watanabe[26], A.A. Watson[c], A. Weindl[41], L. Wiencke[85], H. Wilczyński[70], D. Wittkowski[38], B. Wundheiler[7], B. Yue[38], A. Yushkov[32], O. Zapparrata[14], E. Zas[79], D. Zavrtanik[76,77], M. Zavrtanik[77,76]

—————•—————

[1] Centro Atómico Bariloche and Instituto Balseiro (CNEA-UNCuyo-CONICET), San Carlos de Bariloche, Argentina
[2] Departamento de Física and Departamento de Ciencias de la Atmósfera y los Océanos, FCEyN, Universidad de Buenos Aires and CONICET, Buenos Aires, Argentina
[3] IFLP, Universidad Nacional de La Plata and CONICET, La Plata, Argentina
[4] Instituto de Astronomía y Física del Espacio (IAFE, CONICET-UBA), Buenos Aires, Argentina
[5] Instituto de Física de Rosario (IFIR) – CONICET/U.N.R. and Facultad de Ciencias Bioquímicas y Farmacéuticas U.N.R., Rosario, Argentina
[6] Instituto de Tecnologías en Detección y Astropartículas (CNEA, CONICET, UNSAM), and Universidad Tecnológica Nacional – Facultad Regional Mendoza (CONICET/CNEA), Mendoza, Argentina
[7] Instituto de Tecnologías en Detección y Astropartículas (CNEA, CONICET, UNSAM), Buenos Aires, Argentina
[8] International Center of Advanced Studies and Instituto de Ciencias Físicas, ECyT-UNSAM and CONICET, Campus Miguelete – San Martín, Buenos Aires, Argentina
[9] Laboratorio Atmósfera – Departamento de Investigaciones en Láseres y sus Aplicaciones – UNIDEF (CITEDEF-CONICET), Argentina
[10] Observatorio Pierre Auger, Malargüe, Argentina
[11] Observatorio Pierre Auger and Comisión Nacional de Energía Atómica, Malargüe, Argentina
[12] Universidad Tecnológica Nacional – Facultad Regional Buenos Aires, Buenos Aires, Argentina
[13] University of Adelaide, Adelaide, S.A., Australia
[14] Université Libre de Bruxelles (ULB), Brussels, Belgium
[15] Vrije Universiteit Brussels, Brussels, Belgium
[16] Centro Federal de Educação Tecnológica Celso Suckow da Fonseca, Petropolis, Brazil
[17] Instituto Federal de Educação, Ciência e Tecnologia do Rio de Janeiro (IFRJ), Brazil
[18] Universidade de São Paulo, Escola de Engenharia de Lorena, Lorena, SP, Brazil
[19] Universidade de São Paulo, Instituto de Física de São Carlos, São Carlos, SP, Brazil
[20] Universidade de São Paulo, Instituto de Física, São Paulo, SP, Brazil
[21] Universidade Estadual de Campinas, IFGW, Campinas, SP, Brazil
[22] Universidade Estadual de Feira de Santana, Feira de Santana, Brazil
[23] Universidade Federal de Campina Grande, Centro de Ciencias e Tecnologia, Campina Grande, Brazil
[24] Universidade Federal do ABC, Santo André, SP, Brazil
[25] Universidade Federal do Paraná, Setor Palotina, Palotina, Brazil
[26] Universidade Federal do Rio de Janeiro, Instituto de Física, Rio de Janeiro, RJ, Brazil
[27] Universidade Federal do Rio de Janeiro (UFRJ), Observatório do Valongo, Rio de Janeiro, RJ, Brazil
[28] Universidade Federal Fluminense, EEIMVR, Volta Redonda, RJ, Brazil
[29] Universidad de Medellín, Medellín, Colombia
[30] Universidad Industrial de Santander, Bucaramanga, Colombia

[31] Charles University, Faculty of Mathematics and Physics, Institute of Particle and Nuclear Physics, Prague, Czech Republic
[32] Institute of Physics of the Czech Academy of Sciences, Prague, Czech Republic
[33] Palacky University, Olomouc, Czech Republic
[34] CNRS/IN2P3, IJCLab, Université Paris-Saclay, Orsay, France
[35] Laboratoire de Physique Nucléaire et de Hautes Energies (LPNHE), Sorbonne Université, Université de Paris, CNRS-IN2P3, Paris, France
[36] Univ. Grenoble Alpes, CNRS, Grenoble Institute of Engineering Univ. Grenoble Alpes, LPSC-IN2P3, 38000 Grenoble, France
[37] Université Paris-Saclay, CNRS/IN2P3, IJCLab, Orsay, France
[38] Bergische Universität Wuppertal, Department of Physics, Wuppertal, Germany
[39] Karlsruhe Institute of Technology (KIT), Institute for Experimental Particle Physics, Karlsruhe, Germany
[40] Karlsruhe Institute of Technology (KIT), Institut für Prozessdatenverarbeitung und Elektronik, Karlsruhe, Germany
[41] Karlsruhe Institute of Technology (KIT), Institute for Astroparticle Physics, Karlsruhe, Germany
[42] RWTH Aachen University, III. Physikalisches Institut A, Aachen, Germany
[43] Universität Hamburg, II. Institut für Theoretische Physik, Hamburg, Germany
[44] Universität Siegen, Department Physik – Experimentelle Teilchenphysik, Siegen, Germany
[45] Gran Sasso Science Institute, L'Aquila, Italy
[46] INFN Laboratori Nazionali del Gran Sasso, Assergi (L'Aquila), Italy
[47] INFN, Sezione di Catania, Catania, Italy
[48] INFN, Sezione di Lecce, Lecce, Italy
[49] INFN, Sezione di Milano, Milano, Italy
[50] INFN, Sezione di Napoli, Napoli, Italy
[51] INFN, Sezione di Roma "Tor Vergata", Roma, Italy
[52] INFN, Sezione di Torino, Torino, Italy
[53] Istituto di Astrofisica Spaziale e Fisica Cosmica di Palermo (INAF), Palermo, Italy
[54] Osservatorio Astrofisico di Torino (INAF), Torino, Italy
[55] Politecnico di Milano, Dipartimento di Scienze e Tecnologie Aerospaziali , Milano, Italy
[56] Università del Salento, Dipartimento di Matematica e Fisica "E. De Giorgi", Lecce, Italy
[57] Università dell'Aquila, Dipartimento di Scienze Fisiche e Chimiche, L'Aquila, Italy
[58] Università di Catania, Dipartimento di Fisica e Astronomia "Ettore Majorana", Catania, Italy
[59] Università di Milano, Dipartimento di Fisica, Milano, Italy
[60] Università di Napoli "Federico II", Dipartimento di Fisica "Ettore Pancini", Napoli, Italy
[61] Università di Palermo, Dipartimento di Fisica e Chimica "E. Segrè", Palermo, Italy
[62] Università di Roma "Tor Vergata", Dipartimento di Fisica, Roma, Italy
[63] Università Torino, Dipartimento di Fisica, Torino, Italy
[64] Benemérita Universidad Autónoma de Puebla, Puebla, México
[65] Unidad Profesional Interdisciplinaria en Ingeniería y Tecnologías Avanzadas del Instituto Politécnico Nacional (UPIITA-IPN), México, D.F., México
[66] Universidad Autónoma de Chiapas, Tuxtla Gutiérrez, Chiapas, México
[67] Universidad Michoacana de San Nicolás de Hidalgo, Morelia, Michoacán, México
[68] Universidad Nacional Autónoma de México, México, D.F., México
[69] Universidad Nacional de San Agustin de Arequipa, Facultad de Ciencias Naturales y Formales, Arequipa, Peru
[70] Institute of Nuclear Physics PAN, Krakow, Poland
[71] University of Łódź, Faculty of High-Energy Astrophysics,Łódź, Poland
[72] Laboratório de Instrumentação e Física Experimental de Partículas – LIP and Instituto Superior Técnico – IST, Universidade de Lisboa – UL, Lisboa, Portugal
[73] "Horia Hulubei" National Institute for Physics and Nuclear Engineering, Bucharest-Magurele, Romania
[74] Institute of Space Science, Bucharest-Magurele, Romania
[75] University Politehnica of Bucharest, Bucharest, Romania
[76] Center for Astrophysics and Cosmology (CAC), University of Nova Gorica, Nova Gorica, Slovenia
[77] Experimental Particle Physics Department, J. Stefan Institute, Ljubljana, Slovenia

[78] Universidad de Granada and C.A.F.P.E., Granada, Spain
[79] Instituto Galego de Física de Altas Enerxías (IGFAE), Universidade de Santiago de Compostela, Santiago de Compostela, Spain
[80] IMAPP, Radboud University Nijmegen, Nijmegen, The Netherlands
[81] Nationaal Instituut voor Kernfysica en Hoge Energie Fysica (NIKHEF), Science Park, Amsterdam, The Netherlands
[82] Stichting Astronomisch Onderzoek in Nederland (ASTRON), Dwingeloo, The Netherlands
[83] Universiteit van Amsterdam, Faculty of Science, Amsterdam, The Netherlands
[84] Case Western Reserve University, Cleveland, OH, USA
[85] Colorado School of Mines, Golden, CO, USA
[86] Department of Physics and Astronomy, Lehman College, City University of New York, Bronx, NY, USA
[87] Michigan Technological University, Houghton, MI, USA
[88] New York University, New York, NY, USA
[89] University of Chicago, Enrico Fermi Institute, Chicago, IL, USA
[90] University of Delaware, Department of Physics and Astronomy, Bartol Research Institute, Newark, DE, USA
[91] University of Wisconsin-Madison, Department of Physics and WIPAC, Madison, WI, USA

—–

[a] Louisiana State University, Baton Rouge, LA, USA
[b] also at University of Bucharest, Physics Department, Bucharest, Romania
[c] School of Physics and Astronomy, University of Leeds, Leeds, United Kingdom
[d] now at Agenzia Spaziale Italiana (ASI). Via del Politecnico 00133, Roma, Italy
[e] Fermi National Accelerator Laboratory, Fermilab, Batavia, IL, USA
[f] now at Graduate School of Science, Osaka Metropolitan University, Osaka, Japan
[g] now at ECAP, Erlangen, Germany
[h] Max-Planck-Institut für Radioastronomie, Bonn, Germany
[i] also at Kapteyn Institute, University of Groningen, Groningen, The Netherlands
[j] Colorado State University, Fort Collins, CO, USA
[k] Pennsylvania State University, University Park, PA, USA

Acknowledgments

The successful installation, commissioning, and operation of the Pierre Auger Observatory would not have been possible without the strong commitment and effort from the technical and administrative staff in Malargüe. We are very grateful to the following agencies and organizations for financial support:

Argentina – Comisión Nacional de Energía Atómica; Agencia Nacional de Promoción Científica y Tecnológica (ANPCyT); Consejo Nacional de Investigaciones Científicas y Técnicas (CONICET); Gobierno de la Provincia de Mendoza; Municipalidad de Malargüe; NDM Holdings and Valle Las Leñas; in gratitude for their continuing cooperation over land access; Australia – the Australian Research Council; Belgium – Fonds de la Recherche Scientifique (FNRS); Research Foundation Flanders (FWO); Brazil – Conselho Nacional de Desenvolvimento Científico e Tecnológico (CNPq); Financiadora de Estudos e Projetos (FINEP); Fundação de Amparo à Pesquisa do Estado de Rio de Janeiro (FAPERJ); São Paulo Research Foundation (FAPESP) Grants No. 2019/10151-2, No. 2010/07359-6 and No. 1999/05404-3; Ministério da Ciência, Tecnologia, Inovações e Comunicações (MCTIC); Czech Republic – Grant No. MSMT CR LTT18004, LM2015038, LM2018102, CZ.02.1.01/0.0/0.0/16_013/0001402, CZ.02.1.01/0.0/0.0/18_046/0016010 and CZ.02.1.01/0.0/0.0/17_049/0008422; France – Centre de Calcul IN2P3/CNRS; Centre National de la Recherche Scientifique (CNRS); Conseil Régional Ile-de-France; Département Physique Nucléaire et Corpusculaire (PNC-IN2P3/CNRS); Département Sciences de l'Univers (SDU-INSU/CNRS); Institut Lagrange de Paris (ILP) Grant No. LABEX ANR-10-LABX-63 within the Investissements d'Avenir Programme Grant No. ANR-11-IDEX-0004-02; Germany – Bundesministerium für Bildung und Forschung (BMBF); Deutsche Forschungsgemeinschaft (DFG); Finanzministerium Baden-Württemberg; Helmholtz Alliance for Astroparticle Physics (HAP); Helmholtz-Gemeinschaft Deutscher Forschungszentren (HGF); Ministerium für Kultur und Wissenschaft des Landes Nordrhein-Westfalen; Ministerium für Wissenschaft, Forschung und Kunst des Landes Baden-Württemberg; Italy – Istituto Nazionale di Fisica Nucleare (INFN); Istituto Nazionale di Astrofisica (INAF); Ministero dell'Universitá e della Ricerca (MUR); CETEMPS Center of Excellence; Ministero degli Affari Esteri (MAE), ICSC Centro Nazionale di Ricerca in High Performance Computing, Big Data and Quantum Computing, funded by European Union NextGenerationEU, reference code CN_00000013; México – Consejo Nacional de Ciencia y Tecnología (CONACYT) No. 167733; Universidad Nacional Autónoma de México (UNAM); PAPIIT DGAPA-UNAM; The Netherlands – Ministry of Education, Culture and Science; Netherlands Organisation for Scientific Research (NWO); Dutch national e-infrastructure with the support of SURF Cooperative; Poland – Ministry of Education and Science, grants No. DIR/WK/2018/11 and 2022/WK/12; National Science Centre, grants No. 2016/22/M/ST9/00198, 2016/23/B/ST9/01635, 2020/39/B/ST9/01398, and 2022/45/B/ST9/02163; Portugal – Portuguese national funds and FEDER funds within Programa Operacional Factores de Competitividade through Fundação para a Ciência e a Tecnologia (COMPETE); Romania – Ministry of Research, Innovation and Digitization, CNCS-UEFISCDI, contract no. 30N/2023 under Romanian National Core Program LAPLAS VII, grant no. PN 23 21 01 02 and project number PN-III-P1-1.1-TE-2021-0924/TE57/2022, within PNCDI III; Slovenia – Slovenian Research Agency, grants P1-0031, P1-0385, I0-0033, N1-0111; Spain – Ministerio de Economía, Industria y Competitividad (FPA2017-85114-P and PID2019-104676GB-C32), Xunta de Galicia (ED431C 2017/07), Junta de Andalucía (SOMM17/6104/UGR, P18-FR-4314) Feder Funds, RENATA Red Nacional Temática de Astropartículas (FPA2015-68783-REDT) and María de Maeztu Unit of Excellence (MDM-2016-0692); USA – Department of Energy, Contracts No. DE-AC02-07CH11359, No. DE-FR02-04ER41300, No. DE-FG02-99ER41107 and No. DE-SC0011689; National Science Foundation, Grant No. 0450696; The Grainger Foundation; Marie Curie-IRSES/EPLANET; European Particle Physics Latin American Network; and UNESCO.

PoS(ICRC2023)438